Available online at www.sciencedirect.com
ScienceDirect
Journal of Power Sources 176 (2008) 31–38
JOURNAL OF POWER SOURCES
www.elsevier.com/locate/jpowsour

Influence of through-lamella grain growth on ionic conductivity of plasma-sprayed yttria-stabilized zirconia as an electrolyte in solid oxide fuel cells

Ya-Zhe Xing, Chang-Jiu Li *, Cheng-Xin Li, Guan-Jun Yang

State Key Laboratory for Mechanical Behavior of Materials, School of Materials Science and Engineering, Xi'an Jiaotong University, Xi'an, Shaanxi 710049, PR China

Received 8 August 2007; received in revised form 10 October 2007; accepted 10 October 2007
Available online 18 October 2007

Abstract

The development of a cost-effective fabrication method for stabilized zirconia electrolyte for the most advanced tubular solid oxide fuel cell (SOFC) remains the most important challenge for the commercialization of an SOFC power generation system. Atmospheric plasma spraying is expected to be a promising alternative to other costly electrolyte processing methods. The problem with the plasma-sprayed ceramic coating is the limited interface bonding of the lamellar structure, which reduces the ionic conductivity of stabilized zirconia deposits to one-fifth of the comparable bulk. Continuous growth of columnar grains across splat–splat interfaces has been achieved through control of the substrate surface temperature which affects spreading of molten droplets. These cross-splats columnar grains lead to improved bonding between lamellae. Measurements over the temperature range of 600–1000 °C have shown that the microstructural changes result in a significant increase of ionic conductivity of the yttria-stabilized zirconia deposit (by a factor of about 3). A change in activation energy at about 750 °C was observed for coatings deposited with two different sets of spray conditions. This change is associated with a switch of the predominant ion conduction path from grain boundary to intragrain with increasing temperature.

Keywords: Atmospheric plasma spraying; Yttria-stabilized zirconia; Lamellar structure; Ionic conductivity

1. Introduction

Stabilized zirconia is the most commonly used electrolyte material in solid oxide fuel cells (SOFCs) because of its excellent mechanical strength and outstanding thermal/chemical stabilities in both oxidizing and reducing atmospheres. The most advanced SOFCs employ zirconia-based electrolytes, specifically yttria-stabilized zirconia (YSZ) [1–3]. In order to improve the performance of SOFCs, it is necessary to use electrolyte materials with high ionic conductivity and minimum thickness. Due to the limited ionic conductivity of zirconia, however, SOFCs with a zirconia electrolyte must be operated at high temperatures (800–1000 °C) to reduce Ohmic losses effectively. Moreover, the ionic conductivity, which determines the Ohmic loss of the electrolyte layer [4], is also significantly influenced by its microstructure [5,6].

The electrolyte layer can be fabricated by different routes [7]. Reducing the cost of fabrication of the electrolyte layer is a critical challenge for commercialization of SOFCs [2]. A tubular SOFC with a zirconia-based electrolyte layer deposited by electrochemical vapor deposition (EVD) has exhibited superior output performance [2]. However, the high cost of EVD drives the development of alternative processes for the production of the YSZ layer.

Plasma spraying is proposed as a cheap alternative for producing the electrolyte layer. Atmospheric plasma spraying (APS), due to its relatively high deposition efficiency, flexibility and easy automation, has become a promising candidate for a low-cost process for electrolyte preparation [2,9,10]. Although vacuum plasma spraying (VPS) has been employed to deposit zirconia-based electrolytes for SOFCs and excellent cell perfor-

* Corresponding author. Tel.: +86 29 82660970; fax: +86 29 83237910.
E-mail address: licj@mail.xjtu.edu.cn (C.-J. Li).

0378-7753/$ – see front matter © 2007 Elsevier B.V. All rights reserved.
doi:10.1016/j.jpowsour.2007.10.031

mance has been reported [8], its higher cost compared with APS limits its application to the fabrication of SOFCs.

The primary problem with plasma-sprayed ceramic electrolyte arises from its lamellar structure with poor interface bonding [11,12]. The discontinuous interlamellar interfaces cut off oxygen ion transportation channels and hence reduce the effective ionic conductivity [13]. Our previous studies have revealed that the mean bonding ratio at the interfaces between lamellae is less than 1/3 of the total apparent interface area [11,13–15]. For as-sprayed YSZ electrolyte, during operation of SOFC, oxygen ions move along a direction perpendicular to the lamellae. The lamellar structure leads to a significant drop in the ionic conductivity of as-sprayed YSZ, to about 1/10 to 1/4 of the bulk value [12,16]. The low ionic conductivity certainly reduces the performance of the assembled SOFC. Zirconia-based electrolyte layer deposition by plasma spraying therefore requires further significant improvements in the lamellar interface bonding.

Based on our previous systematic investigation, it is difficult to increase the bonding ratio of the YSZ deposit produced by the conventional coating deposition to more than 1/3. This is due to the fact that the surface temperature of the previously deposited splat upon which the subsequent molten droplets spread cannot be significantly increased by the spreading melt. Furthermore, the wetting of the spreading melt to the splat surface is insufficient to create chemical bonding at the interface. This is ascribed to the fact that the short heating duration means that most particles attain a temperature of around the melting point of the materials involved [17]. On the other hand, we believe that the splat surface temperature can be increased significantly by keeping the substrate at a chosen high temperature during deposition. In this way it may be possible to increase the lamellar interface bonding.

Zirconia-based ceramics are also widely employed as coating materials for thermal barriers [18–20]. In this case poor interface bonding with low thermal conductivity [21] benefits thermal barrier effects [22]. It was found that cracks in the ceramic coating were introduced when an alumina coating was prepared at high substrate temperatures of 370–570 °C [23]. These cracks can improve the stability of a thermal barrier coating [24]. Moreover, it was evident from the result reported by Heintze and Uematsu [25] that the trans-lamellar grain growth can occur at a further high preheating temperature. Jung et al. [26,27], Guo et al. [28–30] and Tricoire et al. [31] have recently observed trans-lamellar columnar grain growth by increasing the substrate temperature during plasma spray deposition of YSZ. Most of these investigations were directed towards the formation of segmentation cracks in order to accommodate the thermal strain in thermal barrier coatings during operation. It was considered that the trans-lamellar grain growth may significantly increase the inter-lamellar bonding and consequently improve the ionic conductivity of plasma-sprayed YSZ coatings. However, no literature has been found dealing with the influence of continuous columnar grain structures on the ionic conductivity of stabilized zirconia coatings for SOFCs.

In this work, prior to deposition of an YSZ coating by plasma spraying, the substrate was preheated to a temperature greater than 800 °C. We have characterized the ionic conductivity of the deposits measured along a direction perpendicular to lamellae in comparison with the as-sprayed deposit using a conventional synthetic route. The influence of microstructural changes of the YSZ coating on its ionic conductivity was investigated.

2. Experimental

Fuse-crushed 8 mol% Y_2O_3–ZrO_2 (8YSZ) powder (Fujimi Co., Japan) was used as feedstock. The particle size range is 5–25 μm. The 8YSZ was deposited by a commercial plasma spray system (80 kW class). The plasma torch was operated at 38.5 kW. The pressures of primary gas Ar and secondary gas H_2 were fixed at 0.8 and 0.4 MPa, respectively. The flow rates of Ar and H_2 were 47 and 5 l min^{-1}, respectively. The powder was fed into a plasma jet using an internal powder port. The torch–substrate distance during deposition was 80 mm. A robot was used to drive the plasma torch back and forth across the substrate surface. An air jet attached to the torch and oriented toward the substrate was employed to cool the sample.

Two kinds of deposits, YSZ-L and YSZ-C, have been prepared. YSZ-L was deposited by following the conventional spray routine, with air cooling and a low substrate temperature, while YSZ-C was deposited on a stainless steel substrate at a high substrate temperature. Aluminum was employed as the substrate material for the preparation of YSZ-L. After spraying, the aluminum substrate was dissolved away using sodium hydroxide to obtain a freestanding YSZ-L deposit about 500 μm thick for ionic conductivity measurements.

By contrast, YSZ-C was deposited on to a stainless steel substrate preheated to 800 °C by a flame torch directed on to the back of the substrate. The substrate temperature was monitored using a pyrometer (RAYRPM30L3U, Raytek, USA). The layers of YSZ-C, about 500 μm thick, were deposited in only one powder stream pass using a low torch traverse speed and with no air jet cooling. Due to the different thermal expansion coefficients of YSZ and stainless steel the deposited layer became detached from the substrate after it was cooled to room temperature.

Both YSZ-L and YSZ-C deposits were polished using a precision lapping/polishing machine (UNIPOL-802, Shenyang, China) under identical polishing conditions. The microstructure of the deposits was characterized by scanning electron microscopy (SEM). To examine the columnar structure and interface bonding, the deposits were also fractured in a direction perpendicular to the deposit surface. The fractured surface was examined using SEM. The phases of both 8YSZ powder and coatings were characterized by X-ray diffraction (XRD).

The ionic conductivities of the samples were measured using both ac and dc methods as described elsewhere [32]. The dc measurements were performed using a potentiostat (TD3691, Tianjing, China) and ac measurements carried out by impedance testing with a Wide-Range Frequency Response Analyzer (TD4020, Tianjing, China) together with the potentiostat. Platinum slurry was pasted on both sides of the freestanding circular YSZ sample in an active area 11 mm diameter. The pasted sample was dried at 100 °C for 30 min, then heated to 850 °C at a heating rate of 5 °C min^{-1} and held for 30 min. The

platinum reference and counter electrodes were connected to one side of the sample, while the working electrode was connected to the other side. According to the linear relation between current and potential difference, the resistivity and ionic conductivity of the 8YSZ deposits were measured.

3. Results

3.1. Microstructure of YSZ coatings

The microstructure of two deposits is shown in Fig. 1. It is clear that the apparent porosity of the 8YSZ coating deposited by the conventional route was greater than that of the deposit plasma-sprayed with substrate preheating. However, the lamellar structure could not be clearly observed for the deposit formed by the conventional route (Fig. 1(a)) even though the deposit should be composed of lamellae. This is due to the limitation of microscopy for the direct observation of the coating microstructure [33]. Large voids are visible (Fig. 1(a)). It is believed that most of these voids resulted from the removal of ceramic particles during the polishing process owing to poor bonding at lamellar interfaces [14]. By comparison, the YSZ-C deposits display a microstructure with few voids, as shown in Fig. 1(b). This suggests improved lamellar interface bonding for the YSZ-C deposits formed with a high substrate temperature because better interface bonding can prevent the removal of particles. As a result, these deposits exhibited a relatively dense microstructure compared with YSZ-L.

To reveal the state of interlamellar bonding for deposits prepared with different substrate preheating temperatures, each was fractured along a direction perpendicular to the surface and the microstructure of the fractured surface examined by SEM. Fig. 2(c) and (d) shows typical microstructures of a fractured 8YSZ deposit sprayed on to a preheated substrate (YSZ-C) in comparison with YSZ-L (Fig. 2(a) and (b)). The columnar grain structure in a direction perpendicular to the lamellar plane is clearly observed in individual splats. Although local bonding is evident at some interfaces in the YSZ-L sample, as indicated by arrow A, most lamellar interfaces are not bonded together, as indicated by arrow B. Moreover, vertical cracks are present in splats, as indicated by arrow C. Those cracks are typical in plasma-sprayed ceramic splats.

On the other hand, the microstructure of the YSZ-C sample shows that most splats were bonded together. This is the most significant feature of its microstructure compared with YSZ-L. Long columnar grains were observed through the coating thickness. This clearly indicates epitaxial growth of columnar grains across splat interfaces when the surface temperature of the pre-deposited splat is greater than 800 °C, although some nonbonded interfaces (arrow B) and vertical cracks (arrow C) are also evident. Moreover, the voids resulting from trapped gas and incomplete flattening of droplets at the periphery zones of solidified splat can also be observed within the coatings, as indicated by arrow D.

Table 1
Ionic conductivity of 8YSZ coatings measured from 600 to 1000 °C

Temperature (°C)		600	700	800	900	1000
Conductivity ($S\,m^{-1}$)	YSZ-L	0.0385	0.187	0.669	1.63	3.48
	YSZ-C	0.113	0.521	2.23	5.25	9.86
Relative conductivity		2.94	2.79	3.34	3.22	2.84

The relative conductivity is the ratio of the conductivities of YSZ-C samples to those of YSZ-L samples.

3.2. Influence of deposition conditions on the ionic conductivity of plasma-sprayed YSZ deposits

The ionic conductivities of both types of 8YSZ sample, measured as a function of temperature, are shown in Fig. 3. It is clear that the ionic conductivity of YSZ-C is higher than that of YSZ-L. Table 1 shows the mean ratio of the ionic conductivity of YSZ-C samples to those of YSZ-L samples at several temperatures. Clearly, the ionic conductivity has been improved by a factor of about 3 when the substrate is preheated to 800 °C. Such a significant improvement in the ionic conductivity is mainly

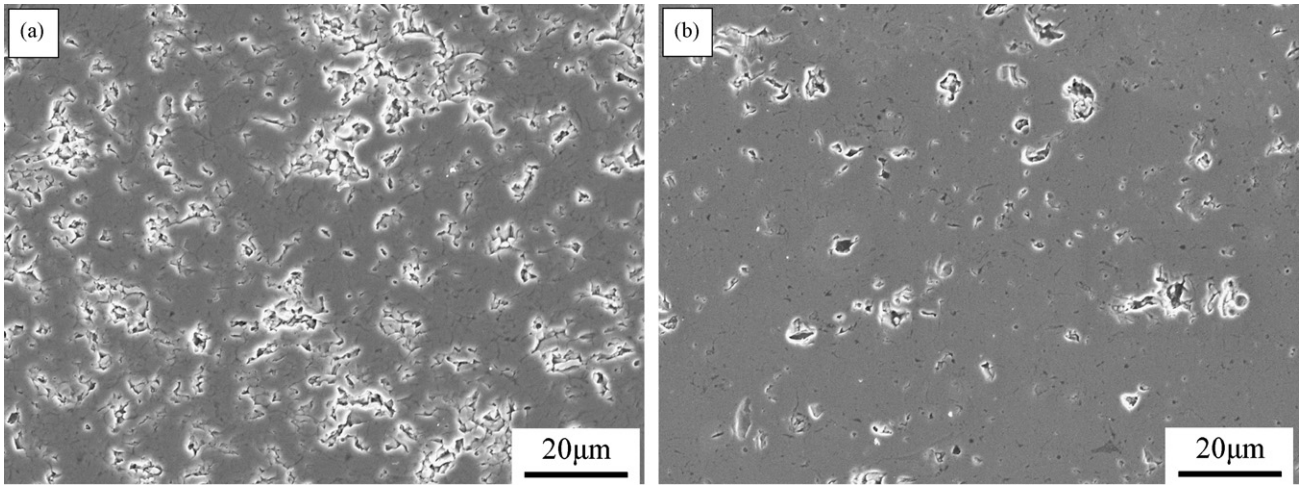

Fig. 1. Cross-sectional microstructure of two 8YSZ deposits plasma-sprayed at different substrate surface temperatures. (a) YSZ-L sample deposited at room temperature and (b) YSZ-C deposited at high temperature.

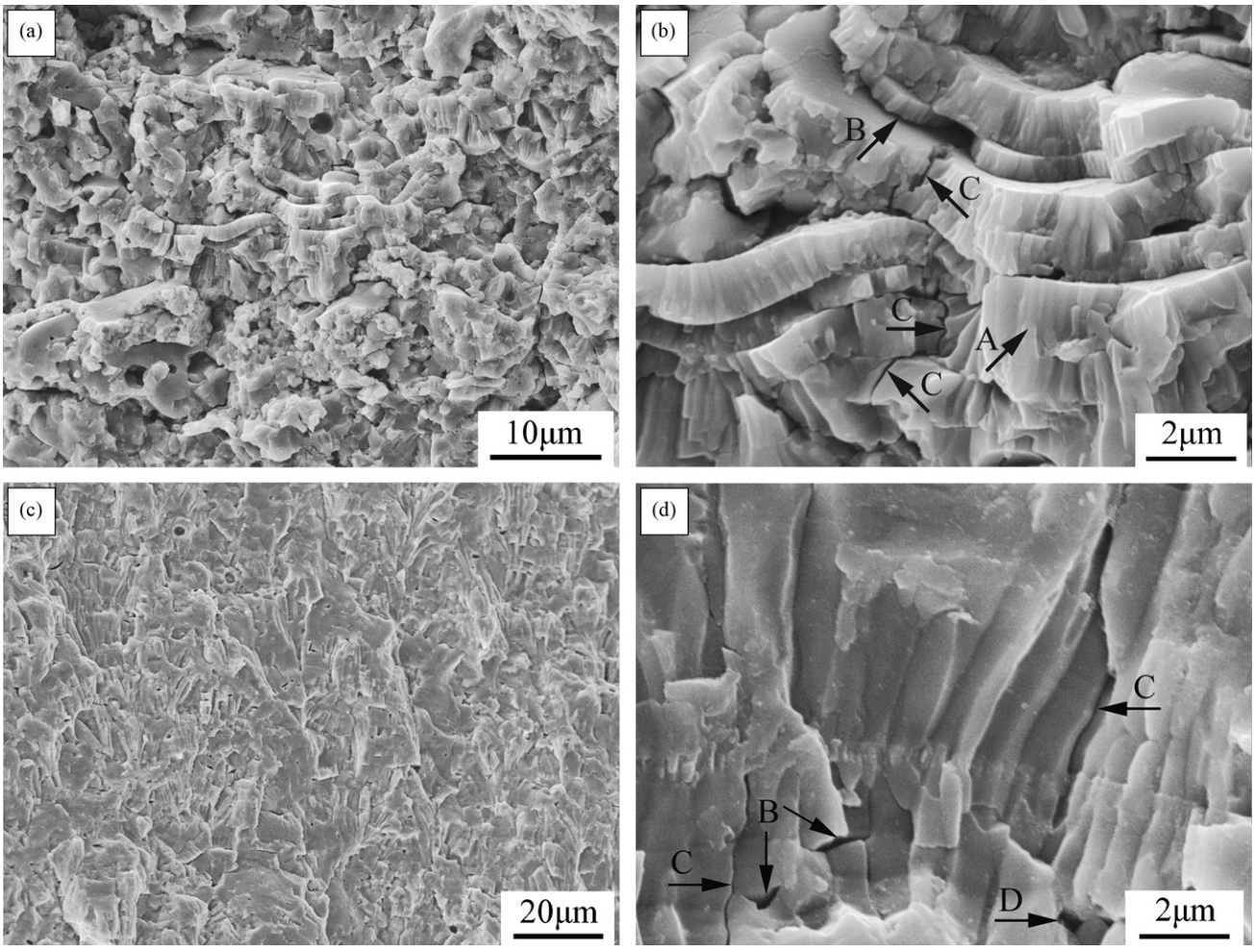

Fig. 2. Microstructures of the fractured 8YSZ deposits plasma-sprayed at different substrate surface temperatures. (a) and (b) YSZ-L samples deposited at room temperature; (c) and (d) YSZ-C samples deposited at high temperature. (a) and (c) low magnification; (b) and (d) high magnification.

attributed to the change in the microstructure of the deposits, as shown in Fig. 2.

From Fig. 3 a plot of $\log \sigma T$ versus $1/T$ gives two straight lines which intersect at a temperature of around 750 °C for both samples. This is consistent with the results reported previously;

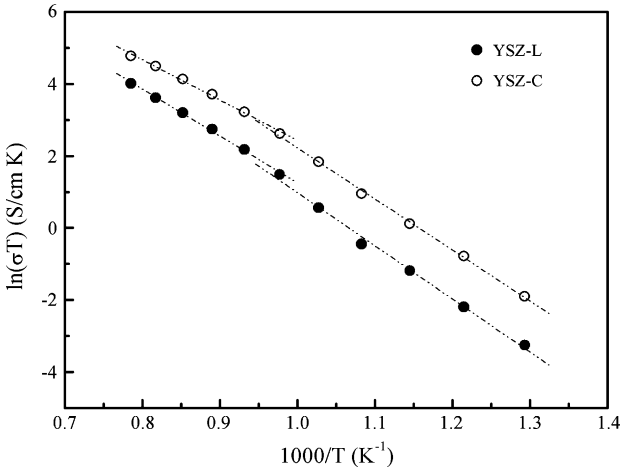

Fig. 3. Ionic conductivity of two 8YSZ deposits vs. temperature.

the change of the slope represents a change of the activation energy [32], which can be calculated as follows [34]:

$$\sigma T = A \exp\left(-\frac{E_a}{kT}\right) \quad (1)$$

where σ is the ionic conductivity, A is the pre-exponential factor, E_a is the activation energy for ionic conductivity, k is the Boltzmann constant and T is the temperature. The activation energy of YSZ-L in the high temperature regime is about 1.12 eV, whereas in low temperature range it is about 1.27 eV. For YSZ-C, the activation energy in the high temperature regime is about 0.96 eV, whereas at low temperatures it becomes 1.22 eV.

4. Discussion

4.1. Influence of surface temperature on the microstructure of deposited coatings

Plasma-sprayed ceramic coatings exhibit lamellar structures with poor lamellar interface bonding. Generally, a columnar microstructure is present in individual plasma-sprayed ceramic splats due to their rapid cooling and solidification as the droplets

impinge on the substrate. McPherson [35] postulated a bonding ratio of about 20% for plasma-sprayed Al_2O_3 coating by supposing that the relative Young's modulus of the ceramic coating to the bulk is proportional to the lamellar interface bonding ratio. The dominance of the limited interface bonding on the thermal conductivity of plasma-sprayed YSZ coatings was also addressed by McPherson [21]. Recent studies reported that poor interface bonding plays an important role in determining the properties and performance of many coatings [12]. Therefore, control of the coating microstructure, especially lamellar interface bonding, is fundamentally important for controlling the properties of the coating.

Some previous studies [11,14–16] have pointed out that the lamellar bonding ratio for conventional thermally sprayed ceramic coatings is less than 1/3. On the other hand, those studies suggested that the coating surface temperature dominates the bonding of the spreading splat with the underlying splats. However, in the case of plasma-sprayed ceramic particles, due to their relatively low temperature and rapid cooling upon impingement, it is difficult to maintain a high splat surface temperature for the impact of subsequent droplets. Increasing the substrate temperature could therefore be effective in keeping the splat surface at a high temperature. Recent investigations of thermal barrier YSZ coatings provide evidence that the splats deposited on a surface with a high temperature bond pretty well with the underlying splats [30]. To attain the direct experimental evidence, we maintained in this study a high splat surface temperature by preheating the substrate to 800 °C. It clearly shows significantly improved lamellar bonding. This is consistent with recent reports by Guo et al. [28–30] and Tricoire et al. [31]. The SEM observation in the present study suggests that most splats are well bonded together through epitaxial grain growth across lamellar interfaces (Fig. 2(d)). Further investigation is needed to clarify the mechanisms of formation of such bonding pertinent to solidification process of spreading splat.

4.2. Relationship between microstructure and ionic conductivity of plasma-sprayed YSZ coatings

The present test showed the ionic conductivity to be 0.0348 S cm^{-1} for the plasma-sprayed YSZ-L deposit at 1000 °C. This is only 22% of the ionic conductivity of sintered bulk (about 0.16 S cm^{-1}) [1].

The ionic conductivity of plasma-sprayed stabilized zirconia deposits is usually measured using a four-probe approach [8,36]. From the results reported by Schiller et al. [8], the ionic conductivity of their vacuum plasma-sprayed 8YSZ deposit was 0.073 S cm^{-1} at 1000 °C. With APS 7YSZ coating, an ionic conductivity of 0.06 S cm^{-1} at 1000 °C was reported [36]. Due to the limited thickness of the deposit, the data reported in the literature are the ionic conductivities along the lamellar direction. Our recent measurements have shown that the ionic conductivity of plasma-sprayed YSZ deposits in a direction parallel to the lamellae is about twice that in the perpendicular direction. This means that the ionic conductivities perpendicular to the lamellar interface for the YSZ deposits as reported in the above literature would be about 0.036 and 0.03 S cm^{-1} at 1000 °C, respectively. These values agree well with the data measured for YSZ-L samples in the present study. Compared with the ionic conductivity of 0.16 S cm^{-1} reported by Yamamoto [1] for 8YSZ bulk at 1000 °C, the ionic conductivity of YSZ-L samples is only about 1/5 of the bulk material. This result is consistent with our previous findings [13,37].

During operation of SOFCs, oxygen ion transfers from the cathode to the anode across a zirconia-based electrolyte layer in a direction perpendicular to the electrolyte lamellae in the deposit. The existence of substantial nonbonded interface areas cuts off many of the direct ion transport pathways. The ionic conductivity of the deposit would be decreased due to the reduction of the effective conduction area. Moreover, limited bonding across the interface and small splat thickness give rise to bending of the conduction pathways of ions and induce an additional contact resistance [39]. This makes the ratio of the effective ionic conductivity of plasma-sprayed YSZ to that of corresponding bulk material even lower than the mean interface bonding ratio, which is less than 1/3 for the plasma-sprayed ceramic deposit [11,16,38].

When YSZ is deposited on to a surface preheated to a temperature greater than 800 °C, most interfaces between adjacent lamellae are bonded together. This microstructure feature allows oxygen ions to transfer directly across the interface and significantly reduce the resistance. As a result, the ionic conductivity of the YSZ deposit layer is increased significantly, by a mean factor of about 3 compared with that deposited by the conventional route. Moreover, the crystalline structure will influence the ionic conductivity of YSZ deposits as was observed for the thermal conductivity of plasma-sprayed YSZ [21]. Fig. 4 shows the XRD patterns of two YSZ deposits compared with that of the starting powder. It confirms that the two deposits show the same cubic crystalline structure as that of the powder. Therefore, the significant increase of ionic conductivity of the YSZ-C deposit compared with YSZ-L must be attributed to a remarkable improvement in lamellar interface bonding. The YSZ-C sample has an ionic conductivity 62% of the sintered bulk. This difference may be attributed to the existence of voids and limited

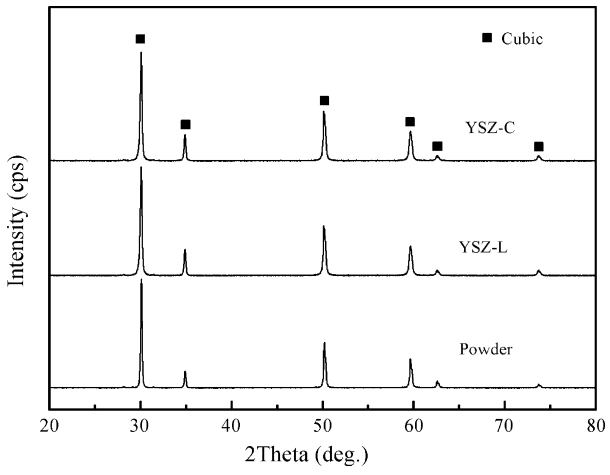

Fig. 4. XRD patterns of two 8YSZ samples deposited at different substrate surface temperatures compared with 8YSZ powder.

nonbonding areas in the deposit, as shown in Fig. 2(d), and also differences in the compositions of the materials.

4.3. Temperature dependence of ionic conductivity for 8YSZ coatings

As shown in Fig. 3, a curvature is observed for Arrhenius plots of $\log \sigma T$ versus $1/T$ at about 750 °C, and the activation energy as evaluated by the slope of Arrhenius plots at low temperature is greater than that at high temperature. This phenomenon has also been reported for zirconia- and ceria-based systems by several investigators [40–43] although the temperature where the change in activation energy takes place is different with different systems. As previous studies [32,40,43] suggested, the change in activation energy with temperature is possibly associated with a change of the predominant ion conduction mechanism from grain boundary to intragrain with the increase of temperature. In order to further examine this phenomenon, the data for grain boundary and intragrain conductivities for both YSZ-L and YSZ-C deposits, as shown in Fig. 5, were measured by ac impedance spectroscopy using the model reported by Kosacki et al. [40] and Zhang et al. [44].

It can be seen that the grain boundary conductivity is higher than the intragrain conductivity in the high temperature range for both samples. This means that at high temperatures the intragrain conductivity dominates the total conductivity. In this case, the apparent ionic conductivity of the deposits depends on the effective conducting area which is determined by the interface bonding condition. The previous study yielded a lamellar interface bonding ratio of about 32% for plasma-sprayed YSZ coating [38]. We suppose that the reduction of ionic conductivity contributed by contact resistance is responsible for the reduction to 22% of the relative conductivity with respect to sintered bulk from the mean bonding ratio of 32%. Moreover, with a high bonding ratio the contact resistance can be neglected. The approximate threefold increase in ionic conductivity of YSZ-C compared with YSZ-L implies that the lamellar interface bonding ratio has increased. As a result, it is suggested that the lamellar interface in the YSZ sample deposited at high temperature has almost been bonded together. In the high temperature range, the ionic conductivity depends on the intragrain conductivity. This indicates that the ionic conductivity is proportional to the effective bonding area. Table 1 shows an almost threefold increase in ionic conductivity of YSZ-C compared with YSZ-L regardless of the temperature. This provides further evidence that the increase of the ionic conductivity of the YSZ deposit results from the significant improvement of lamellar interface bonding, which notably increases the effective conducting area. The difference of ionic conductivity of the YSZ deposit from that of the sintered bulk is attributed to the occasional voids and nonbonded interfaces formed in the deposits, as shown in Fig. 2(d).

4.4. Activation energy for ion conduction

According to the intragrain–intergrain model [45], ion conduction will be dominated by the intragrain resistance in the high temperature regime and dominated by grain boundary resistance at lower temperatures. On the other hand, the oxygen vacancy trapping mechanism suggests that at high temperatures the ion conduction is also controlled by intragrain resistance, while in the low temperature range it is controlled by migration of free oxygen vacancies and also by thermal dissociation of defect-associates. Therefore, we considered that in the high temperature range the dominant factor governing ion transportation within zirconia-based electrolytes is intragrain resistance for both monocrystalline and polycrystalline materials. Accordingly, for zirconia-based electrolyte with identical compositions, the activation energy for ion transportation is independent of the grain boundary resistance at high temperature. However, at lower temperatures, the ion transportation is mainly controlled by the grain boundary resistance, thermal dissociation of defect-associates and intragrain resistance. The non-linear Arrhenius behavior reported by many investigators [43–49] for both monocrystalline and polycrystalline materials, demonstrates that the intragrain resistance is not the dominant factor for ion conduction in zirconia-based electrolytes at low temperatures. With monocrystalline YSZ free of grain boundaries, the

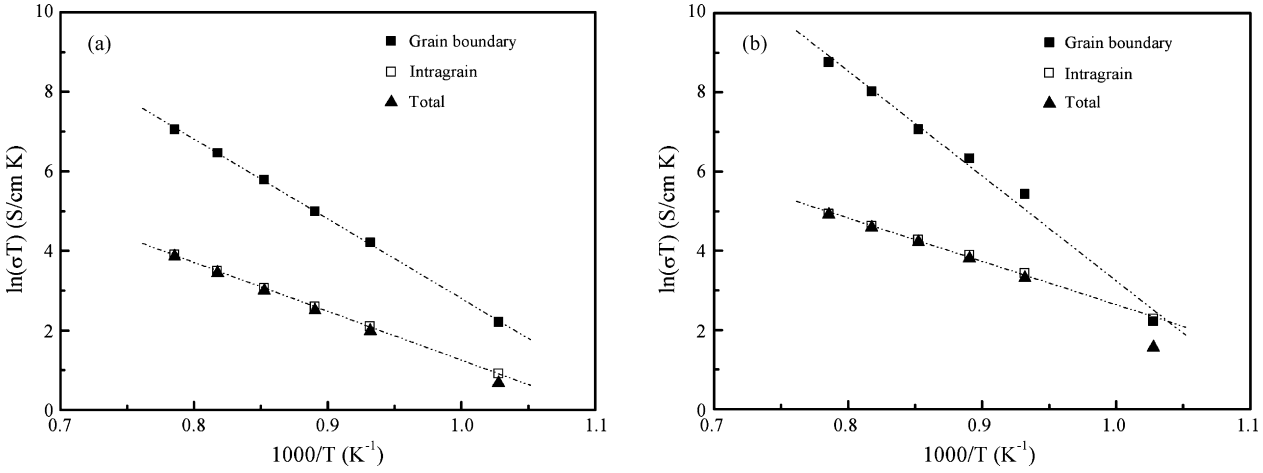

Fig. 5. Temperature dependence of intragrain and intergrain boundary conductivities determined by ac measurements for (a) YSZ-L and (b) YSZ-C.

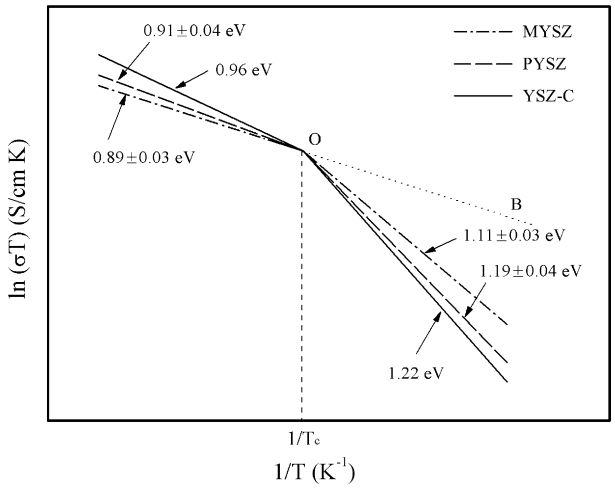

Fig. 6. Schematic diagram of the change of activation energy of monocrystalline and polycrystalline yttria-stabilized zirconia compared with YSZ deposits vs. temperature. The data for monocrystalline 9.5 mol% yttria-stabilized zirconia (MYSZ) are from Ref. [43], and those of polycrystalline 8 mol% yttria-stabilized zirconia (PYSZ) are from Ref. [50]. T_c values differ in the range from 550 to 750 °C in different reports.

dominant factor for ion transportation at low temperature is the thermal dissociation of defect-associates. With polycrystalline YSZ, the dominant factor depends on the relative values of the activation energy for ion transportation across grain boundaries and the activation energy for thermal dissociation of defect-associates. In other words, when the activation energy for ion transportation across grain boundaries is larger than that for thermal dissociation of defect-associates the grain boundary resistance will be dominant, whereas grain boundary resistance will not dominate the ion conduction. For monocrystalline yttria-stabilized zirconia (MYSZ), as shown in Fig. 6 and as reported by Filal et al. [43], the activation energy for ion migration is 0.89 eV (OB) in the high temperature range, while it rises to 1.11 eV in the low temperature range. This can be explained by a mechanism involving the trapping of oxygen vacancies due to the absence of grain boundaries. As a result, the 0.22 eV increase in activation energy can be attributed to the supplementary energy for the thermal dissociation of the defect-associates. Moreover, the activation energy in the low temperature regime for YSZ-C in the present work reached about 1.22 eV, which is larger than that for MYSZ. Therefore, in the low temperature range the ion conduction in YSZ-C is still dominated by grain boundary resistance. Because plasma-sprayed YSZ deposit consists primarily of polycrystalline material its ionic conducting behavior is similar to polycrystalline bulk YSZ. Therefore, the activation energies of plasma-sprayed deposits are comparable to those of sintered bulk with identical composition. The activation energy of the YSZ deposit in the low temperature range is comparable to that reported by Gong et al. [50].

5. Conclusions

Plasma spraying is expected to be a cost-effective process for manufacturing stabilized zirconia electrolytes for SOFCs. A significant reduction of ionic conductivity by comparison with the bulk material was clearly observed for 8YSZ deposits produced by APS in conventional route due to the presence of a lamellar structure with poor interface bonding. By increasing the surface temperature of the substrate to a sufficiently high level the columnar grains could be grown continuously from underlying splat surface and the interface between splats was almost chemically bonded. This microstructure change led to significant improvements of the ionic conductivity of plasma-sprayed 8YSZ deposit, by a mean factor of about 3 in the range 600–1000 °C. The results also revealed that the surface temperature of the previous deposit on to which spray molten droplets spread dominates the bonding at the interface. The deposition temperature can be controlled through the substrate surface temperature prior to droplet impact.

A change in activation energy for ion conduction at about 750 °C was observed for both deposits. This change is associated with the change in the dominant mechanism for ion conduction from grain boundary to intragrain with increasing of temperature.

Acknowledgements

This work is supported by National Natural Science Foundation of China (Granted No.50671080) and National High Technology Research and Development Program of China (Granted No.2007AA05Z135).

References

[1] O. Yamamoto, Electrochim. Acta 45 (2000) 2423–2435.
[2] M.C. Williams, J.P. Strakey, S.C. Singhal, J. Power Sources 131 (2004) 79–85.
[3] F.J. Gardner, M.J. Day, N.P. Brandon, M.N. Pashley, M. Cassidy, J. Power Sources 86 (2000) 122–129.
[4] S.J. Geng, J.H. Zhu, Z.G. Lu, Scripta Mater. 55 (2006) 239–242.
[5] Y.W. Zhang, S. Jin, Y. Yang, G.B. Li, S.J. Tian, J.T. Jia, C.S. Liao, C.H. Yan, Appl. Phys. Lett. 77 (2000) 3409–3411.
[6] A. Rivera, J. Santamaría, C. León, Appl. Phys. Lett. 78 (2001) 610–612.
[7] J. Will, A. Mitterdorfer, C. Kleinlongel, D. Perednis, L.J. Gauckler, Solid State Ionics 131 (2000) 79–96.
[8] G. Schiller, R.H. Henne, M. Lang, R. Ruckaschel, S. Schaper, Fuel Cell Bull. 3 (2001) 7–12.
[9] C.-J. Li, C.-X. Li, X.-J. Ning, Vacuum 73 (2004) 699–703.
[10] C.-J. Li, C.-X. Li, Y.-Z. Xing, M. Gao, G.-J. Yang, Solid State Ionics 177 (2006) 2065–2069.
[11] A. Ohmori, C.-J. Li, Thin Solid Films 201 (1991) 241–252.
[12] C.-J. Li, A. Ohmori, J. Thermal Spray Technol. 11 (2002) 365–374.
[13] C.-J. Li, X.-J. Ning, C.-X. Li, Surf. Coat. Technol. 190 (2005) 60–64.
[14] A. Ohmori, C.-J. Li, Y. Arata, Trans. Jpn. Weld. Res. Inst. 19 (1990) 259–270.
[15] C.-J. Li, A. Ohmori, Surf. Coat. Technol. 82 (1996) 254–258.
[16] C.-J. Li, A. Ohmori, Y. Arata, in: A. Ohmori (Ed.), Proceedings of 14th International Thermal Spray Conference, Japan High Temperature Society, 1995, pp. 501–506.
[17] P. Fauchais, M. Vardelle, A. Vardelle, J.F. Coudert, Metall. Trans. 20B (1989) 263–276.
[18] R.A. Miller, C.E. Lowell, Thin Solid Films 95 (1982) 265–273.
[19] N.P. Padture, M. Gell, E.H. Jordan, Science 296 (2002) 280–284.
[20] A.G. Evans, D.R. Mumm, J.W. Hutchinson, G.H. Meier, F.S. Pettit, Prog. Mater. Sci. 46 (2001) 505–553.
[21] R. McPherson, Thin Solid Films 112 (1984) 89–95.
[22] M. Okazaki, H. Yamano, Int. J. Fatigue 27 (2005) 1613–1622.

[23] L. Gyenis, A. Grimaud, O. Betoule, M.F. Monerie, P. Fauchais, M. Ducos, Proceedings of 2nd Plasma-Technik-Symposium, Lucerne, Switzerland, June 5–7, 1991, pp. 95–101.
[24] H.B. Guo, H. Murakami, S. Kuroda, Mater. Trans. 47 (2006) 306–309.
[25] G.N. Heintze, S. Uematsu, Surf. Coat. Technol. 50 (1992) 213–222.
[26] I.-H. Jung, K.-K. Bae, M.-S. Yang, S.-K. Ihm, J. Thermal Spray Technol. 9 (2000) 463–477.
[27] I.-H. Jung, J.-S. Moon, K.-C. Song, M.-S. Yang, Surf. Coat. Technol. 180–181 (2004) 454–457.
[28] H.B. Guo, R. Vaβen, D. Stöver, Surf. Coat. Technol. 186 (2004) 353–363.
[29] H.B. Guo, S. Kuroda, H. Murakami, Thin Solid Films 506–507 (2006) 136–139.
[30] H.B. Guo, S. Kuroda, H. Murakami, J. Am. Ceram. Soc. 89 (2006) 1432–1439.
[31] A. Tricoire, M. Vardelle, P. Fauchais, Limoges, F. Braillard, A. Malie, Chatellerault, P. Bengtsson, P. Corbeil-Essone, in: E. Lugscheider (Ed.), Thermal Spray Connects: Explore its Surfacing Potential, Proceedings of the 2005 International Thermal Spray Conference, Basil, Switzerland, 2005, pp. 924–928.
[32] C.-X. Li, C.-J. Li, H.-G. Long, Y.-Z. Xing, H.-L. Liao, C. Coddet, Solid State Ionics 177 (2006) 2149–2153.
[33] C.-J. Li, W.-Z. Wang, Mater. Sci. Eng. A 386 (2004) 10–19.
[34] S.P.S. Badwal, J. Mater. Sci. 18 (1983) 3117–3127.
[35] R. McPherson, Surf. Coat. Technol. 39/40 (1989) 173–181.
[36] T. Okuo, Y. Kaga, A. Momma, Denki Kagaku 64 (1996) 555–561.
[37] X.-J. Ning, C.-J. Li, C.-X. Li, G.-J. Yang, Mater. Sci. Eng. A 428 (2006) 98–105.
[38] W.-Z. Wang, C.-J. Li, K. Sonoya, Yokohama, in: E. Lugscheider (Ed.), Thermal Spray Connects: Explore its Surfacing Potential, Proceedings of the 2005 International Thermal Spray Conference, Basil, Switzerland, 2005, pp. 1506–1510.
[39] F.B. Bowden, D. Tabor, The Friction and Lubrication of Solids, Oxford University Press, London, 1964, pp. 34–42.
[40] I. Kosacki, H.U. Anderson, Y. Mizutani, K. Ukai, Solid State Ionics 152–153 (2002) 431–438.
[41] D.D. Edwards, J.-H. Hwang, S.J. Ford, T.O. Mason, Solid State Ionics 99 (1997) 85–93.
[42] R. Chiba, T. Ishiil, F. Yoshimura, Solid State Ionics 91 (1996) 249–256.
[43] M. Filal, C. Petot, M. Mokchah, C. Chateau, J.L. Carpentier, Solid State Ionics 80 (1995) 27–35.
[44] C. Zhang, C.-J. Li, G. Zhang, X.-J. Ning, C.-X. Li, H. Liao, C. Coddet, Mater. Sci. Eng. B 137 (2007) 24–30.
[45] J.E. Bauerle, J. Hrizo, J. Phys. Chem. Solids 30 (1969) 565–570.
[46] A. Cheikh, A. Madani, A. Touati, H. Boussetta, C. Monty, J. Eur. Ceram. Soc. 21 (2001) 1837–1841.
[47] P.S. Manning, J.D. Sirman, R.A. De Souza, J.A. Kilner, Solid State Ionics 100 (1997) 1–10.
[48] X. Guo, R. Waser, Prog. Mater. Sci. 51 (2006) 151–210.
[49] J.A. Kilner, C.D. Waters, Solid State Ionics 6 (1982) 253–259.
[50] J.H. Gong, Y. Li, Z.L. Tang, Y.H. Xie, Z.T. Zhang, Mater. Chem. Phys. 76 (2002) 212–216.